LIQUEFACTION POTENTIAL MAP FOR UTAH COUNTY, UTAH COMPLETE TECHNICAL REPORT
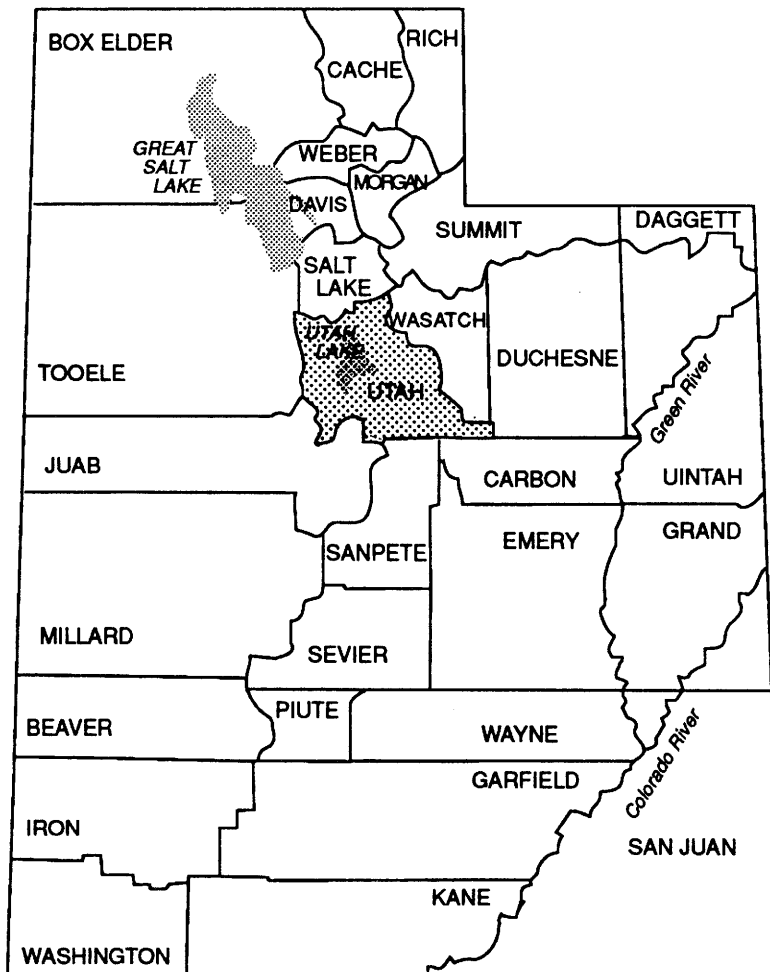
by
Loren R. Anderson
Jeffrey R. Keaton
Jon E. Bischoff

LIQUEFACTION POTENTIAL MAP

for

UTAH COUNTY, UTAH

by

Loren R. Anderson, Jeffrey R. Keaton
and Jon E. Bischoff

Department of Civil and Environmental Engineering
Utah State University
Logan, Utah
and
Dames & Moore Consulting Engineers
Salt Lake City, Utah

May 1986

ACKNOWLEDGMENTS

TABLE OF CONTENTS

TABLE OF CONTENTS (Continued)

LIST OF TABLES

LIST OF FIGURES

LIST OF PLATES

EXECUTIVE SUMMARY

As part of the U.S. Geological Survey's Earthquake Hazard Reduction
program a "Liquefaction Potential Map" has been prepared for Utah
County, Utah. Liquefaction potential was evaluated from existing
subsurface data and from a supplementary subsurface investigation
performed as one of the tasks in this study. All of the data used in
this study are summarized on the base maps presented as Plates 1A to 1D
and 2A to 2D.

For this regional assessment, liquefaction implies liquefaction-
induced ground failure. The liquefaction potential is classified as
high, moderate, low and very low depending on the probability that a
critical acceleration will be exceeded in 100 years. The critical
acceleration for a given location is defined as the lowest value of the
maximum ground surface acceleration required to induce liquefaction.
The categories of high, moderate, low and very low correspond to
probabilities of exceeding the critical acceleration in the ranges of
greater than 50 percent, 10 to 50 percent, 5 to 10 percent and less
than 5 percent, respectively.

The Liquefaction Potential Map on Plates 4A through 4D shows that
for a significant portion of Utah County the probability of exceeding
the critical acceleration in 100 years is greater than 50 percent.
Hence, liquefaction induced ground failure is a significant seismic hazard.
Ground slope information, as well as the subsurface conditions documented
on the Soils and Ground Water Data Map, can be used in combination with
the Liquefaction Potential Map as a means of assessing the type of

ground failure likely to occur. Three slope zones have been identified

from the characteristic failure modes induced by liquefaction during

historic earthquakes (Youd, 1981, personal communication).

At slope gradients less than about 0.5 percent, loss of bearing

capacity is the type of ground failure most likely to be induced by

soil liquefaction. Stratified soil conditions, which existing in Utah

County, provide vertical confinement for liquefiable layers and may

tend to reduce the probability of bearing capacity failures. Buildings

imposing light loads on the subsurface soils may not be affected by

loss of bearing capacity during an earthquake. Heavy buildings, on the

other hand, might be severely affected. Additionally, during earthquakes,

heavy buildings subjected to movement from deformation of the subsurface

soils might cause damage to adjacent lightly-loaded structures.

Buried tanks, even those full of water or gasoline, could "float"

to the surface if the soils surrounding them were to liquefy. For this

to happen, however, the tanks would have to be buried in very thick

deposits of sand. The stratified nature of the soils in Utah County

generally tends to reduce the likelihood of this type of failure.

Slope gradients ranging from about 0.5 percent to about 5.0 percent

tend to fail by lateral spread processes as a result of soil liquefaction.

Evidence exists in Utah County for large lateral spread landslides (see

Plates 1A through 1D). Consequently, it appears that these kinds of

failures have occurred in response to earthquakes within the past few

thousand years.

Lateral spread landslides present the greatest concern because of

the potential consequences. A small amount of movement can do a great

deal of damage. Lifelines (buried utilities) are particularly vulnerable.

A large amount of Utah County falls within the slope range characterized by lateral spread landslides induced by soil liquefaction.

Slopes steeper than about 5 percent tend to fail as flow slides if the mass of soil comprising the slope liquefies. In Utah County, the stratified nature of the geologic materials suggests that flow-type failures are likely to be relatively rare. Instead, translational landslides or lateral spreads are likely to result from liquefaction on slopes steeper than about 5 percent.

It should be emphasized that perched ground water is equal to true ground water with respect to soil liquefaction. Saturated granular material is the chief concern; the source of the saturation is immaterial.

The results of our research on the liquefaction potential of Utah County leads us to conclude that lateral spread landsliding is the type of ground failure most likely to accompany soil liquefaction. The probability of extensive damage due to this type of ground failure is high. All types of structures could be damaged by liquefaction-induced ground failure; lifelines are especially susceptible to damage.

Anderson and Keaton (1986) present a decision matrix that suggests mitigation measures for liquefaction induced ground failure hazards. The matrix considers the rating of the liquefaction zone and the proposed land use of the area.

INTRODUCTION

General

The effects of earthquakes can cause loss of life and costly property
damage; therefore, in areas of high seismic activity, earthquake hazard
reduction must be an important consideration for intelligent land use
planning. Damage during earthquakes can result from surface faulting,
ground shaking, ground failure, generation of large waves (tsunamies
and seiches) in bodies of water, and regional subsidence or downwarping
(Nichols and Buchanan-Banks, 1974). Although all of these causes of
damage need to be considered in reducing earthquake hazards, this
report deals only with liquefaction-induced ground failure.

Ground failure associated with earthquake-induced soil liquefaction
has caused major damage during past earthquakes (Seed, 1979; Youd and
Hoose, 1977). The seismic history of the Wasatch front area in north-
central Utah clearly indicates that ground motion of sufficient intensity
and duration to induce liquefaction of susceptible soils is very likely
to occur in the relatively near future.

Deposits of loose fine sand, highly susceptible to liquefaction,
exist along the Wasatch front (McGregor and others, 1974; Anderson and
others, 1982). Areas of shallow ground water are also widespread (Hely
and others, 1971, Fig. 80). In addition, evidence of liquefaction was
observed following the 1934 Hansel Valley earthquake in Box Elder
County, Utah (Coffman and von Hake, 1973, p. 71) and again following
the Cache Valley earthquake of 1962 (Hill, 1979).

The seismic history, subsurface soil and ground water conditions,
and evidence of liquefaction in Utah indicate that liquefaction is a

1

significant hazard which must be assessed as an important element in seismic hazard reduction planning.

Purpose and Scope of Study

The purpose of this study was to develop a liquefaction potential map for Utah County, Utah. Utah County is located in northern Utah's urban corridor just south of Salt Lake Valley. Utah County contains one of Utah's largest population centers, the Provo-Orem area. The study area extends from the Wasatch Mountains west to and including Cedar and Goshen Valleys as shown on Fig. 1.

The liquefaction potential was evaluated on the basis of subsurface data that was obtained from private engineering consultants, state and local government agencies, and from a supplementary subsurface investigation performed as one of the tasks in this study. The results of the study are summarized on four maps; each map consists of four parts (A, B, C, & D) separating the county into approximate quadrants, northwest, northeast, southwest, and southeast.

The base maps are 50 percent reductions of U.S. Geological Survey 7 1/2-minute topographic quadrangles (a scale of 1:48,000). The four maps are presented in later sections of this report and consist of (1) Selected Geologic Data Map, (2) Soils and Ground Water Data Map, (3) Ground Slope and Critical Acceleration Map and (4) Liquefaction Potential Map.

Boring logs and laboratory data that were collected and developed during the study are maintained in the files of the Civil Engineering Department at Utah State University.
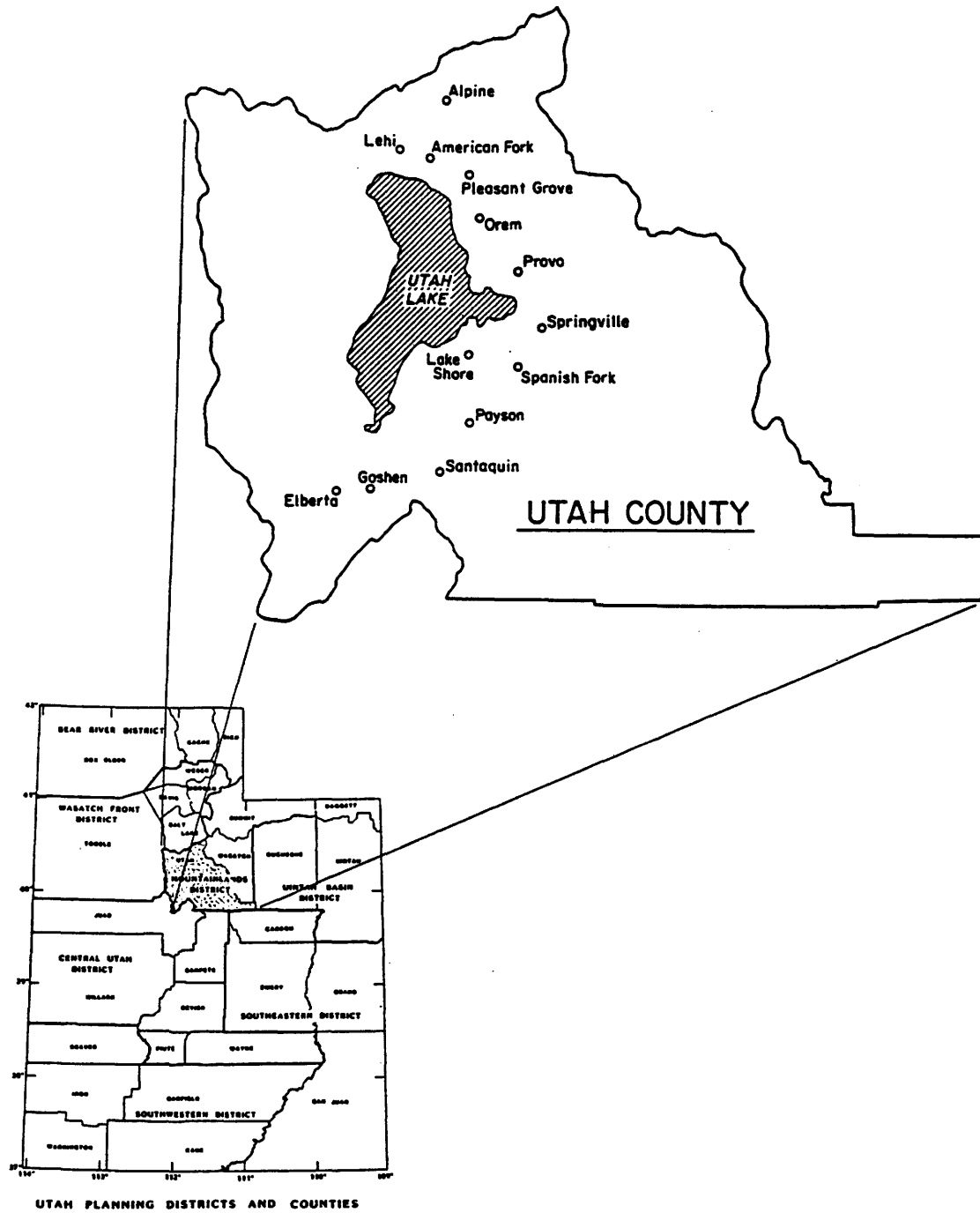
Figure 1. Utah County showing major communities.

Liquefaction-Induced Ground Failure

Loose, saturated fine sand deposits subjected to earthquake shaking can liquefy, losing essentially all shear strength, because pressures are rapidly transferred from the granular structure of the soil to the pore water. If the pore water pressure increases until the intergranular stress is reduced to zero, a condition of "initial liquefaction" is reached (Seed, 1976). For loose sands, this condition is usually accompanied by large deformations and ground failure typically occurs.

Ground failure commonly associated with liquefaction may be manifested in several forms: (1) sand boils, (2) flow landslides, (3) lateral spread landslides, (4) ground oscillation, (5) loss of bearing capacity, (6) buoyant rise of buried structures, (7) ground settlement, and (8) failure of retaining walls (National Research Council, 1985). Youd and others (1975) related flow landslides, lateral spread landslides, and bearing capacity failures to the slope of the ground surface. The most common type of liquefaction-induced ground failure is probably lateral spread landsliding. However, the topographic and geologic conditions of Utah County make all eight types of ground failure possible.

Regional Seismicity

The state of Utah is bisected by the Intermountain Seismic Belt (Fig. 2). The occurrence of earthquakes in the state is common and has been documented since 1850; a plot of the locations of epicenters from July 1962 to June 1978 (Fig. 3) graphically illustrates that earthquakes in Utah are common.

Many known and suspected Quaternary faults have been mapped in Utah (Fig. 4); the Wasatch fault zone is one of the most prominent. The

ARABASZ, SMITH, AND RICHINS — 1979.
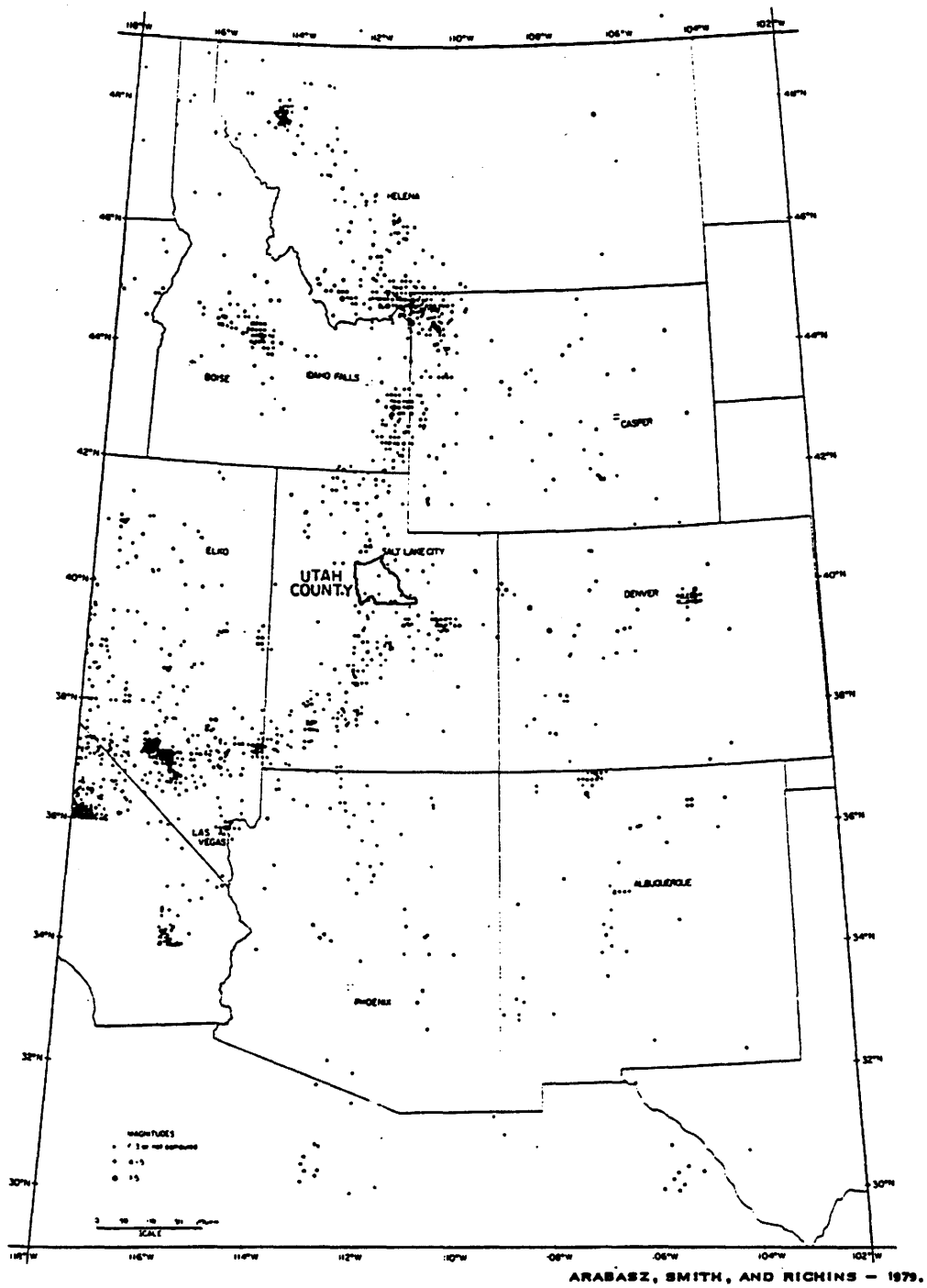
Figure 2.   Intermountain Seismic Belt (1850 – 1974).
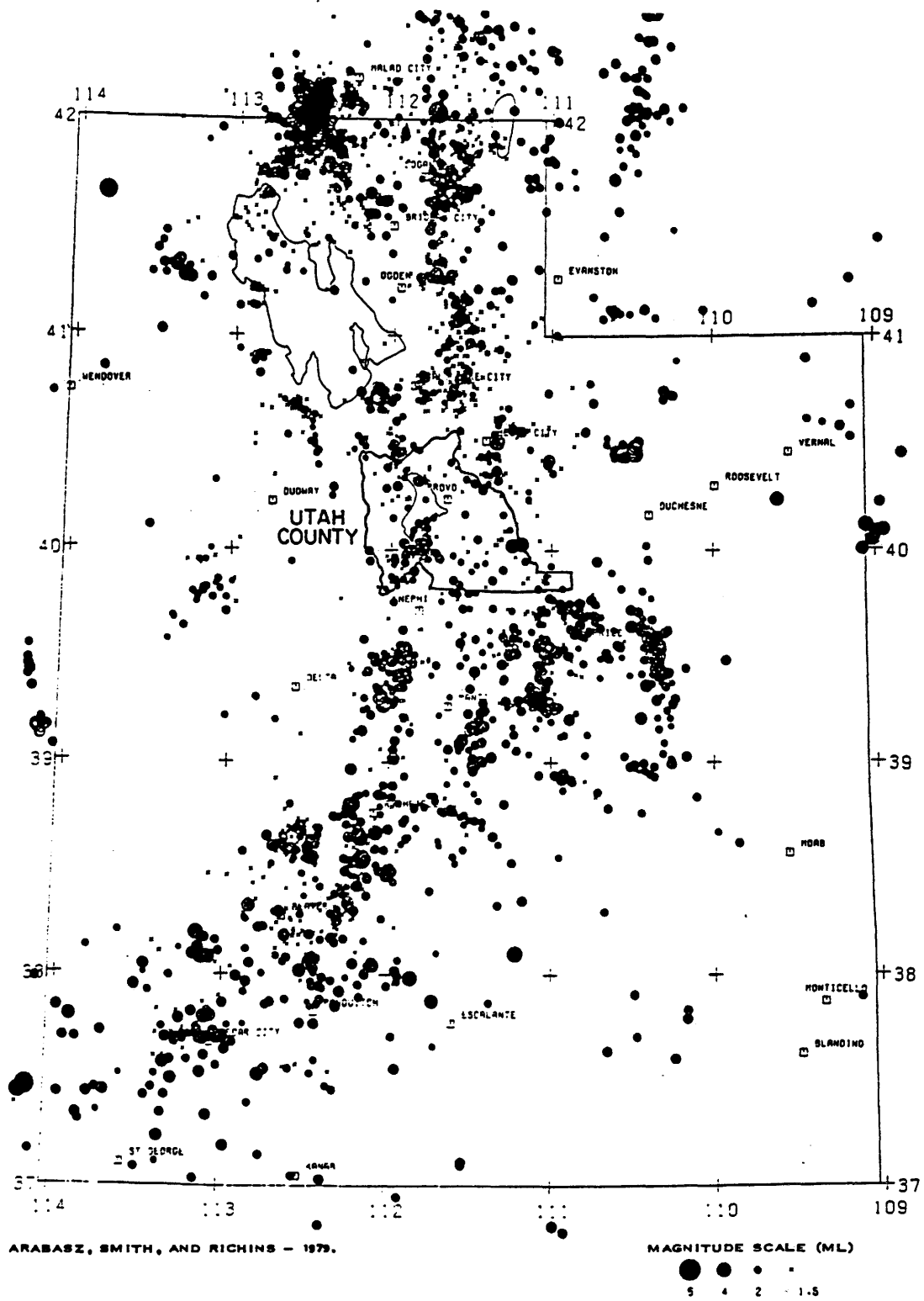
Figure 3. Epicenters in Utah, July 1962 to June 1978.
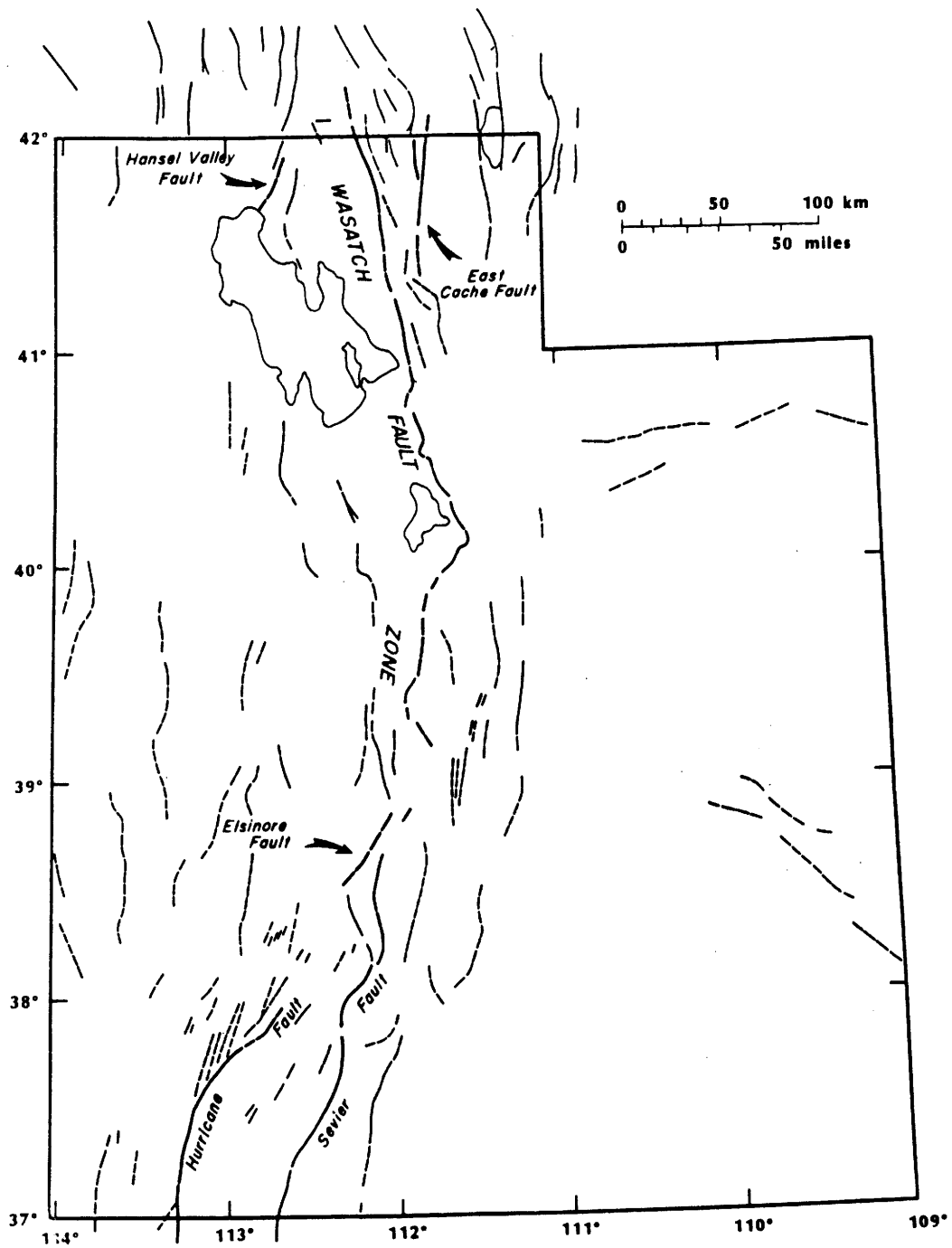
Figure 4. Known and suspected Quaternary faults in Utah (After Arabasz and others, 1979; Anderson and Miller, 1979).

distribution of fault traces (Fig. 4) has a strong relationship with epicenter locations (Fig. 3). Swan and other (1980) investigated the Wasatch fault zone at two sites in the urban corridor of the Wastach front. They estimated that moderate to large magnitude earthquakes (M_L = 6 1/2 to 7 1/2) on the Wasatch fault zone may occur as frequently as 50 to 430 years.

General Subsurface Conditions

Virtually all of the urbanized area of Utah County was inundated by Pleistocene Lake Bonneville, of which the Great Salt Lake and Utah Lake are remnants. Consequently, most of the sediments in Utah County are probably late Pleistocene or younger in age.

The lake bed sediments of the region generally consist of deposits of sand, silt and clay. The liquefiable sand and silt deposits vary in thickness from several millimeters to several meters and occur throughout Utah County. Extensive gravel deposits are present along the east side of the study area on the upper Lake Bonneville shore lines. These gravel deposits are most notable in the Provo River delta region located in the northeast part of the study area approximately in the Orem area.

The ground water table in much of the study area is within a few feet of the ground surface and local areas of artesian conditions are present. In the bench areas along the higher shore lines of Lake Bonneville, the water table is generally much deeper but cases of perched ground water are known to exist possibly in the Mapleton Bench area. Lawn sprinkling and other effects of additional development along the bench areas will probably contribute to the occurrence of perched ground water.

METHODOLOGY

General

Subsurface data was collected for selected sites from throughout

the Utah County study area. Ground surface accelerations required to

induce liquefaction at each site were computed. These acceleration

values are referred to as "critical accelerations." The liquefaction

potential for each site was then classified as high, moderate, low or

very low depending on the probability of the computed "critical"

ground surface acceleration being exceeded in 100 years.

Factors Affecting Liquefaction Potential

The factors affecting liquefaction include soil properties, initial

stress conditions, seismic history and the characteristics of the

earthquake motion. Aside from saturated conditions, the following

factors are considered fundamental: (1) soil type, (2) relative density,

(3) initial confining pressure, (4) intensity and duration of ground

shaking, (5) soil structure and (6) seismic history.

Deposits of loose fine to medium sand with uniform grain size

distributions are generally considered to be the most susceptible to

liquefaction. Soils with more than about 15 percent clay typically

have sufficient cohesive strength that liquefaction will not occur.

Very loose sands are most susceptible to liquefaction while very dense

sands are least susceptible. High confining pressure requires more

stress to initiate liquefaction than does low confining pressure.

Sands that have been subjected to repeated ground shaking without

inducing liquefaction are less susceptible to liquefaction than sands without such a seismic history.

The characteristics of the earthquake motion that affect liquefaction opportunity are the intensity and duration of ground shaking. Consideration of these ground shaking characteristics is important in evaluating liquefaction potential.

Evaluation of Liquefaction Potential

An evaluation of liquefaction potential at a given site by current state of the art methods involves comparing the predicted cyclic stress ratio $(\tau/\sigma_o{}')$ that would be induced by a given design earthquake with the cyclic stress ratio required to induce liquefaction. Figure 5 illustrates this comparison. The predicted cyclic stress ratio can be computed using response analysis techniques or by a simplified procedure based on rigid body theory modified to account for the flexibility of the soil profile (Seed, 1976). The simplified theory for computing the cyclic stress ratio induced by an earthquake is given by Eq. 1.

$$\frac{\tau_{av}}{\sigma_o{}'} \approx 0.65 \frac{a_{max}}{g} \left(\frac{\sigma_o}{\sigma_o{}'}\right) r_d \qquad (1)$$

where, a_{max} = maximum acceleration at ground surface

σ_o = total overburden pressure on sand layer under consideration

$\sigma_o{}'$ = initial effective overburden pressure on sand layer under consideration

r_d = a stress reduction factor varying from a value of 1 at the ground surface to a value of 0.9 at a depth of about 30 ft.

The cyclic stress ratio required to cause liquefaction can be evaluated either by laboratory tests on undisturbed samples or by an
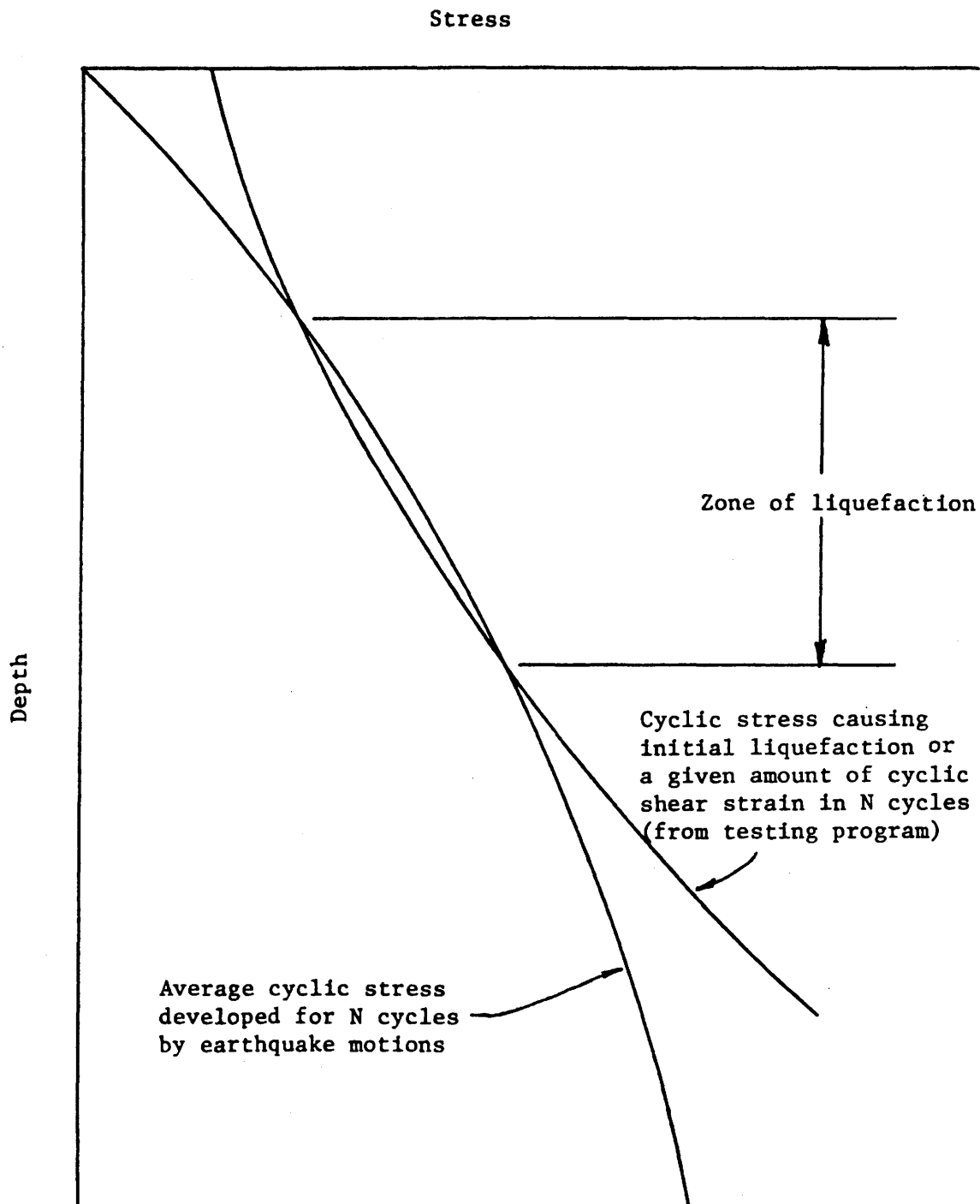
Stress

Figure 5. Method of evaluating liquefaction potential (after Seed and Idriss, 1971).

empirical relationship between some insitu property of the soil and the

cyclic stress ratio required to cause liquefaction. Securing undisturbed

samples of sand for laboratory testing is a very difficult, if not

impossible, task and the use of reconstituted samples would not model

the seismic history or structure of the soil deposit. Therefore, the

use of laboratory tests to evaluate the cyclic stress required to

induce liquefaction in natural deposits is questionable.

Seed, Mori and Chan (1977) have developed an empirical relationship

(shown on Fig. 6) between the cyclic stress ratio required to cause

liquefaction and the standard penetration resistance of the soil.

Seed (1976) points out that the factors that tend to influence

liquefaction susceptibility such as relative density, age of the deposit,

seismic history and soil structure also tend to influence the standard

penetration resistance in a like manner. Although the penetration test

has its shortcomings, if used properly and with judgment, it provides a

convenient and rapid method of evaluating the insitu characteristics of

sand. The standard penetration test also provides a convenient method

to utilize existing data in evaluating liquefaction potential because

in the past the most common method to obtain samples of sand has been

the standard penetration test.

Silty sands ($D_{50} < 0.15$mm) have been found to be less liquefiable

than clean sands ($D_{50} > 0.25$mm) for the same penetration resistance,

Seed and Idriss (1982). Therefore, correlation between field liquefaction

behavior of silty sands and standard penetration resistance has been

developed (Tatsuoka and ers, 1980) and is shown in Figure 7. The

difference in the blow count values between the clean sand and silty

sand curves is about 7.5. Therefore, "for silty sand and silts plotting
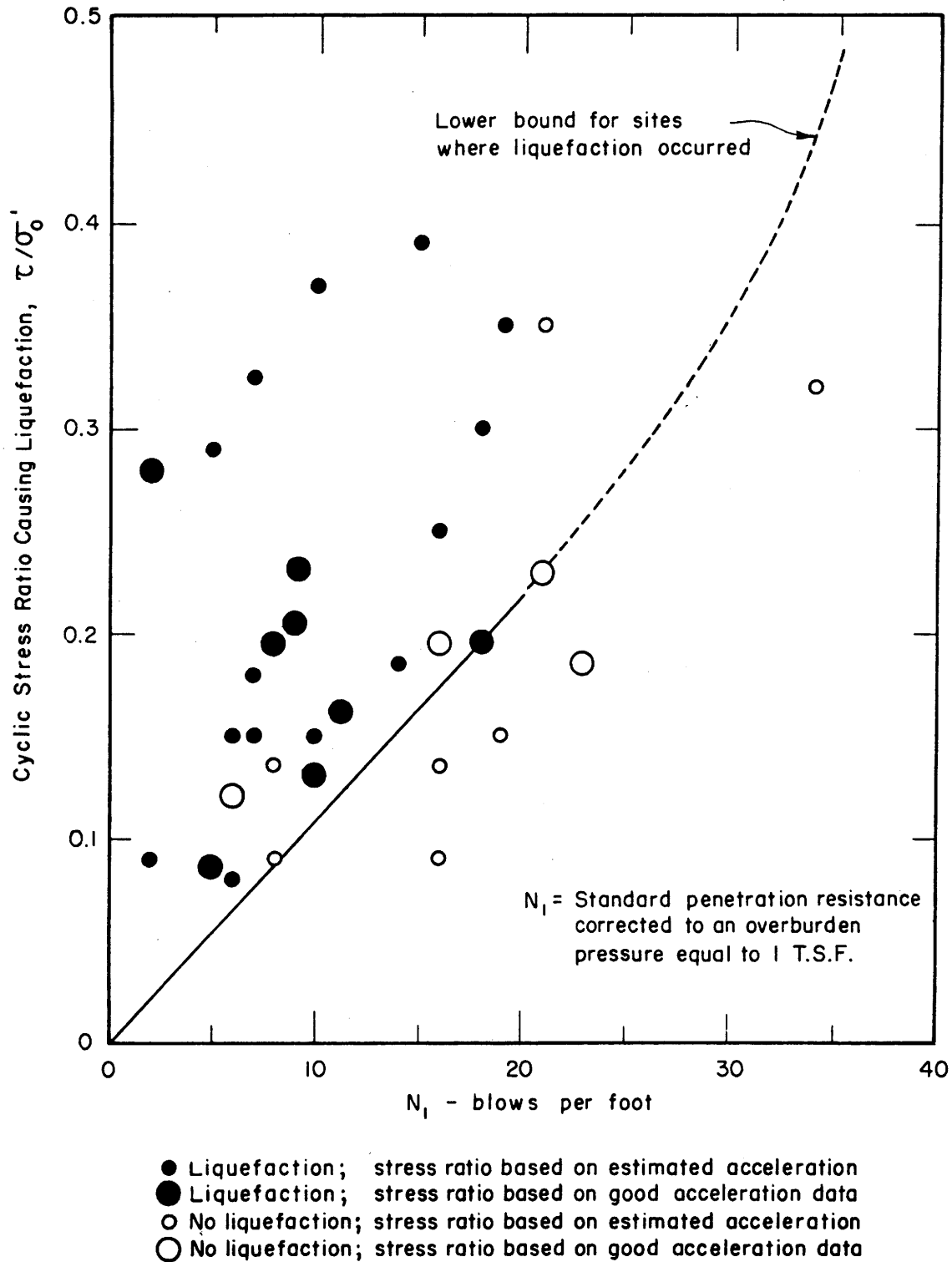
Figure 6. Observed field behavior of sand correlated to cyclic stress ratio and standard penetration resistance (after Seed, Mori and Chan, 1977).
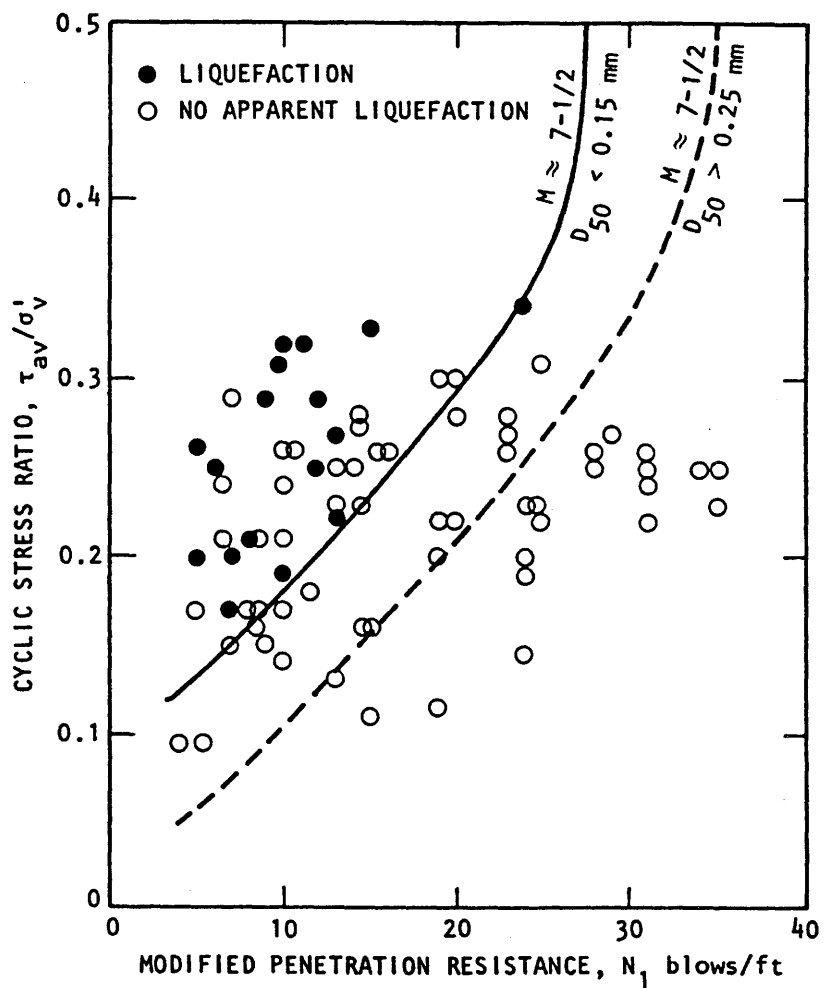
Figure 7. Correlation between field liquefaction behavior
of silty sands (D_{50} > 0.15 mm) under level ground
conditions and standard penetration resistance
(Data after Tokimatsu and Yoshimi, 1981). (From
Seed and Idriss, 1982).

below the A-line and with D_{50} < 0.15mm, use N=(N) + 7.5, and then use the standard correlation curves for sands." (Seed and others, 1983, p. 479).

Gibbs and Holtz (1957) correlated standard penetration resistance with relative density and effective overburden pressure. Their work showed that the standard penetration resistance for a constant relative density was a function of the overburden pressure. Therefore, Seed, Mori and Chan (1977) used a standard penetration resistance corrected to an overburden pressure of one ton per square foot in developing the relationship between standard penetration resistance and the cyclic stress ratio required to cause liquefaction given by Fig. 6. A correction factor must also be used with Figure 7. The correction factor used by Seed, Mori and Chan is based on Gibbs and Holtz work and was suggested by Peck, Hansen and Thornburn (1973). The correction factor is applied as follows:

$$N_1 = C_N \cdot N \tag{2}$$

where,
$$C_N = 1 - 1.25 \log \frac{\sigma_o{}'}{\sigma_1{}'}$$

$\sigma_o{}'$ = effective overburden pressure in tons per square foot where the penetration has a value of N

$\sigma_1{}'$ = one ton per square foot

Correlations for Difference Magnitude Earthquakes

Figures 6 and 7 provide a basis for developing correlations between SPT values and liquefaction characteristics of sands and silty sands for magnitude 7.5 earthquakes. These results have been extended to other magnitude events by noting that the main difference between

different magnitude earthquakes is the number of cycles of stress which they induce (Table 1).

The relationship between cyclic stress ratio and number of cycles required to cause liquefaction is shown in Figure 8. Therefore, by multiplying the 7.5 magnitude boundary curve in Figure 7 by the scaling factors shown in Figure 8, boundary curves separating sites where liquefaction is likely to occur or unlikely to occur may be determined for different magnitudes (Figure 9).

Use of SPT Correlation Charts with CPT Data

The main advantages of the cone penetrometer (CPT) are that it provides information rapidly and it provides a continuous record of penetration resistance. The main disadvantage is that the CPT is accompanied by a very limited data base to provide correlation between soil liquefaction characteristics and CPT values (Seed and others, 1983). The test may be used, however, by establishing correlation between the CPT and SPT values at new sites (Douglas and others, 1981), or by using available SPT-CPT correlations from previously conducted studies.

Cyclic stress ratios required to cause liquefaction can be obtained using the CPT values by either converting these values to SPT N values, then normalizing the N values and using the relationship shown in Figure 9, or by normalizing the Q value by use of the equation:

$$Q_{c1} = Q_c * C \qquad\qquad (3)$$

Then with the Q_{c1} values, Figure 10 may be used directly to obtain the critical cyclic stress ratio (Seed and others, 1983).

Table 1. Earthquake magnitudes and their associated number of
representative cycles (after Seed and Idriss, 1982).

Earthquake Magnitude, M	No. of representative cycles at $0.65\tau_{max}$
8½	26
7½	15
6¾	10
6	5-6
5¼	2-3

NUMBER OF CYCLES TO CAUSE r_u = 100% AND ±5% STRAIN
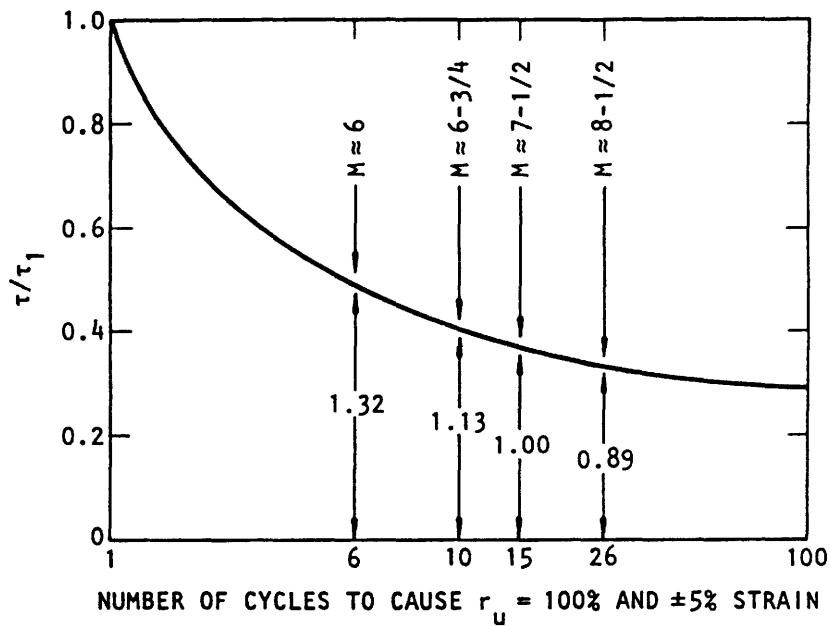
Figure 8. Representative relationship between τ/τ_1 and the
number of cycles required to cause liquefaction
(after Seed and Idriss, 1982).
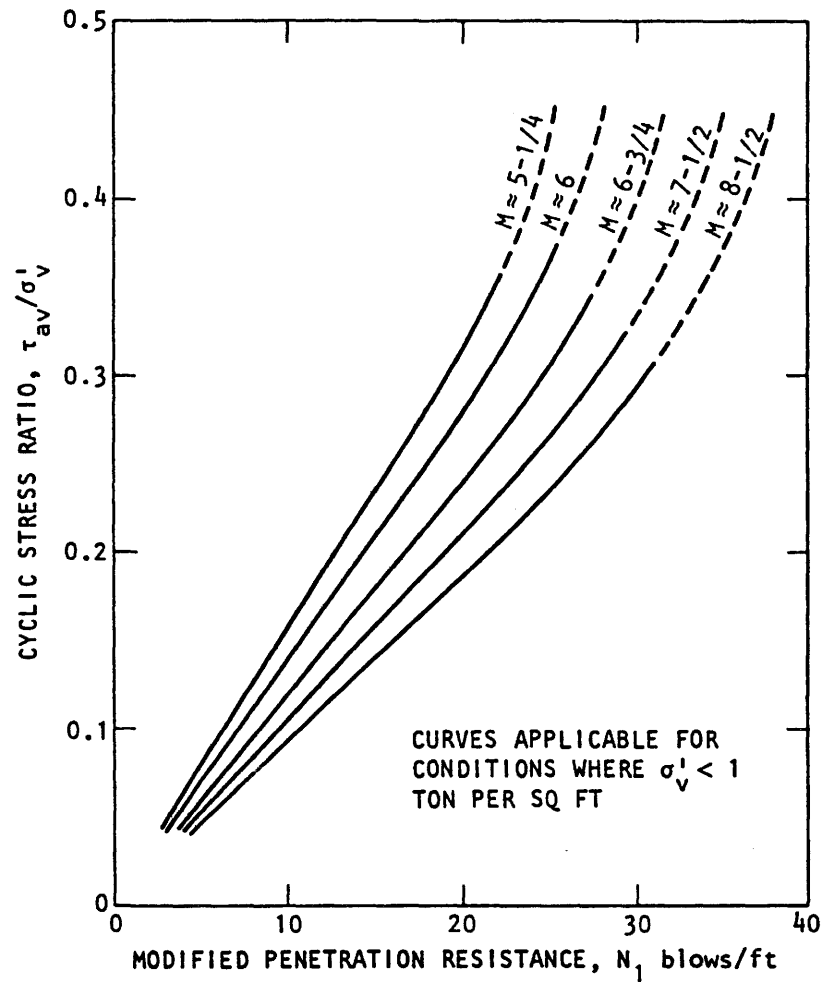
Figure 9. Chart for evaluation of liquefaction potential for sands for different magnitude earthquakes (after Seed and Idriss, 1982).
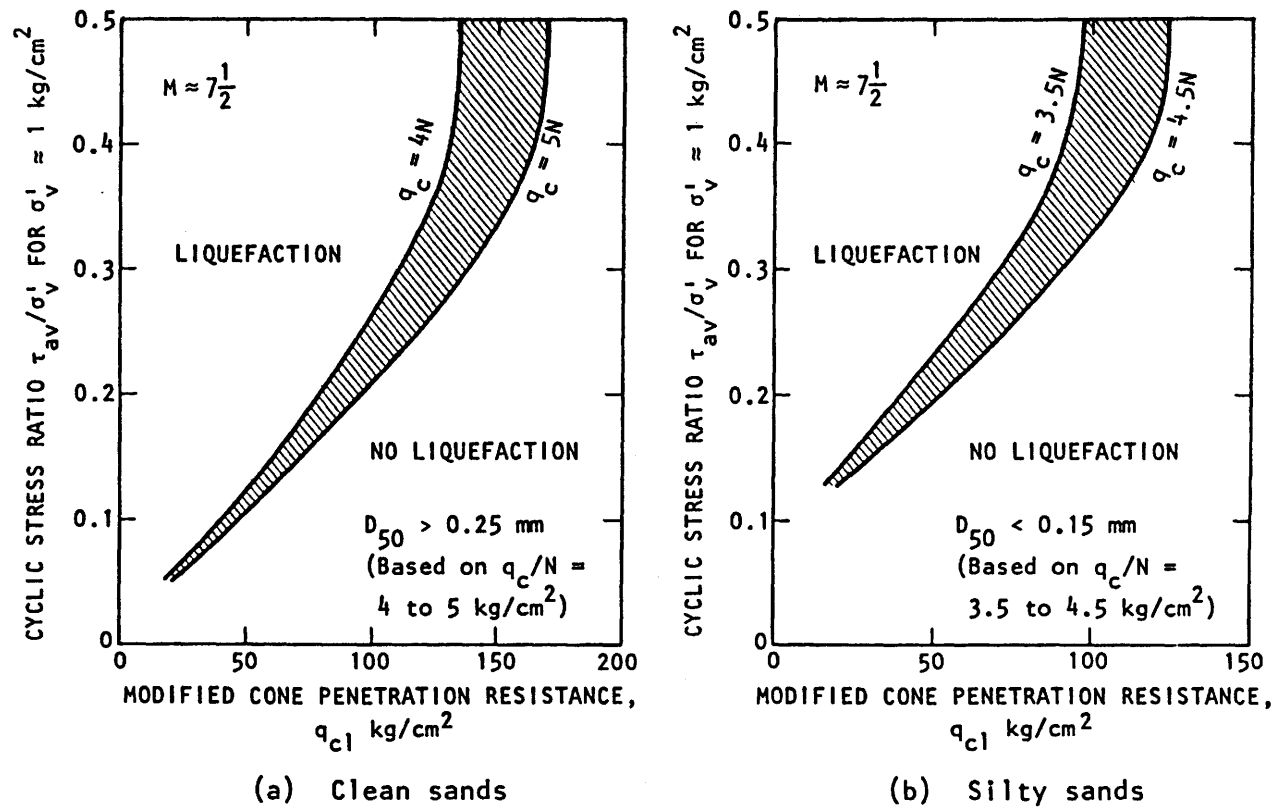
Figure 10.   Correlation between field liquefaction behavior of sands under level ground
conditions and static cone penetration resistance (after Seed and Idriss, 1982).

Liquefaction Potential Based on Critical Acceleration

Qualitative descriptions of the liquefaction potential in the Utah County study area were assigned on the basis of the probability that the computed values of critical acceleration would be exceeded during a 100 year time period. The critical acceleration for a given location is defined as the lowest value of maximum ground surface acceleration required to induce liquefaction.

The standard penetration test data from soil borings and cone penetrometer data in conjunction with Eq. 1 and Figs. 9 and 10 were used to compute the critical acceleration at numerous locations throughout the study area. Equation 1 can be solved for the critical acceleration and stated as:

$$(a_{max})_c = (\frac{\tau_{av}}{\sigma_o'}) (\frac{\sigma_o'}{\sigma_o}) (\frac{1}{0.65 \ r_d}) \qquad (4)$$

where, $(a_{max})_c$ = critical acceleration (ground surface acceleration required to induce liquefaction at a given site)

$(\frac{\tau_{av}}{\sigma_o'})$ = cyclic stress ratio required to cause liquefaction at the given site and obtained from the standard penetration resistance and Figure 6.

σ_o = total overburden pressure at the point where the standard penetration resistance is measured.

σ_o' = effective overburden pressure at the point where the standard penetration resistance is measured.

Note that the cyclic stress ratio, $(\frac{\tau_{av}}{\sigma_o'})$, required to cause liquefaction is computed using Figures 9 and 10 and the standard penetration and cone sounding results from each boring and cone location. The 7 1/2 magnitude curve in Figure 9 was utilized to be consistent with previous

studies and in light of suggestions that the characteristic earthquake for the Wasatch fault is in the 7.0 to 7.5 range.

Judgment was required in assigning critical acceleration values. Generally more than one boring log was available for a given site and many standard penetration values were reported for each boring. Therefore, several critical acceleration values were computed for each boring at each site. A value considered to be representative of the critical acceleration was then assigned to the site. In assigning this representative value, consideration was given to consistency within and between borings, to the soil type and to the limitations of the standard penetration test. A single low critical acceleration value at a site was not considered representative if it was not consistent with other critical acceleration values at the site and in the general area. Computer programs aided in the computation of the critical accelerations.

Critical acceleration values were computed for gravelly sand, sand and silty sand, and for sandy silt with generally less than 15 percent clay-size material and a plastic index less than 5. Since the penetration value is the number of blows required to drive a standard sampler one foot, layers being evaluated must be at least one foot thick. For this reason, borings containing sand layers thinner than one foot could not be assigned acceleration values. However, very limited cone penetrometer data did allow computation of critical acceleration values for sand layers less than 1 foot thick.

As stated above, the liquefaction potential was assigned on the basis of the probability that the critical acceleration would be exceeded in 100 years. The probabilities used in assigning liquefaction potential are presented in Table 2.

Table 2. Liquefaction potential related to
exceedance probability

Probability of Exceeding Critical Acceleration in 100 years	Liquefaction Potential
> 50%	High
10-50%	Moderate
5-10%	Low
< 5%	Very Low

The probability values delineating liquefaction potential were selected partially on the basis of probability limits frequently used in selecting accelerations for structural design purposes. In structural engineering the concept of dual levels of design accelerations has become widely accepted in recent years. This concept first considers an earthquake with a moderate probability of occurrence during the projected lifetime of a structure; the structure should be designed to remain elastic (completely functional) during the earthquake event. The structure as designed for this first event should then be analyzed to estimate its probable response to a larger event which has a smaller probability of occurrence. The structure would be expected to develop ductility (be damaged) during its response to the second and larger motion but not expected to collapse.

The values usually chosen for these two levels of acceleration are (1) the value which has a 50 percent probability of being exceeded during the projected life of the structure (the elastic design motion) and (2) a value close to that which has only a 10 percent probability of being exceeded during the life of the structure (the larger acceleration for which the structure may develop ductility). These probability

values of 50 percent and 10 percent were set as the limits delineating
the high and moderate liquefaction potential categories. A probability
value of 5 percent was then arbitrarily selected to separate low and
very low liquefaction potential. For planning purposes, a 100-year time
period was used.

Other probability limits could have been selected and this would
have some effect on the configuration of liquefaction potential categories
on the map. However, regardless of the probability values used to
define the high, moderate, low and very low classifications, those
selected clearly allow a relative assessment of the liquefaction hazard
within the study area.

Liquefaction Potential Map

Computed critical acceleration values for specific sites were
plotted on a map of the study area. A two-step procedure was then used
to develop the Liquefaction Potential Map. Contours of equal critical
acceleration were first drawn on the basis of the critical acceleration
values. These contours were used to divide the study area into zones
of high, moderate, low and very low liquefaction potential. The contours
represented the critical accelerations that had exceedance probabilities
of 50, 10 and 5 percent in 100 years.

After the liquefaction potential zones were initially identified
from the critical acceleration contours, they were adjusted to reflect
the geology of the area. This adjustment was particularly important
because subsurface data and critical acceleration values were available
only at selected locations and did not necessarily reflect specific

geologic features such as the locations of stream beds and the late

Pleistocene Lake Bonneville shore lines.

Ground Failure Mode

The Liquefaction Potential Map delineates the various liquefaction

potential zones. It can be used in conjunction with soil data and

ground slope maps to predict the probable type of ground failure. Youd

(1978) suggested that the type of ground failure induced by liquefaction

is related to the ground surface slope and proposed the relationships

between ground slope and failure mode shown in Table 3.

Table 3. Ground slope and expected failure mode (after Youd, 1978)

Ground Surface Slope	Failure Mode
< 0.5%	Bearing capacity
0.5 - 5.0%	Lateral spread
> 5.0%	Flow landslide

The thickness and setting of the sand deposit should also be

considered in determining the probable mode of ground failure. For

example, a 1 meter-thick loose sand layer at a depth of 10 meters in an

otherwise clay soil profile is not likely to cause a flow landslide or

a significant bearing capacity failure regardless of the ground surface

slope. However, this condition might induce a translational landslide

in steep slopes or magnify ground surface movement due to ground oscilla-

tion (lurching) in flat areas.

A Ground Surface Slope Map and a Soil Properties Map were prepared

for the study area. These maps can be used in conjunction with the

Liquefaction Potential Map to evaluate the potential for various types of ground surface failure.

GEOTECHNICAL CONDITIONS IN UTAH COUNTY, UTAH

Geology Related to Liquefaction

Introduction

The geology of Utah County is dominated by erosional and depositional features associated with the several still-stands of pluvial lakes which existed in the eastern Great Basin over the past 30,000 or more years. Intermittent displacement along major geologic structures in the Great Basin since early Tertiary time created fault-bounded mountain blocks separated by deep basins (Cook and Berg, 1961, p. 75). The Wasatch fault zone is the dominant structural feature of Utah County.

Geologic materials in Utah County can be characterized into three types: pre-Lake Bonneville materials, Lake Bonneville materials, and post-Lake Bonneville materials. In Utah County, pre-Lake Bonneville materials are not susceptible to liquefaction because they are dense an cemented (indurated). Lake Bonneville materials and post-Lake Bonneville materials exhibit liquefaction potentials ranging from very low to high depending on ground water conditions and proximity to the mountain front. The three types of geologic materials are identified on Plates 1A and 1D, Selected Geologic Data, and are discussed below.

Pre-Lake Bonneville Materials

These materials constitute the Wasatch Range, Traverse Mountains, Lake Mountains, and West Mountains in Utah County and underlie lake deposits in the basin. The exposed rocks in Utah County range in age

from Precambrian to Quaternary and range in composition from volcanic
rocks to limestone (Baker, 1964, 1972, 1973; Backer and Crittenden,
1961; Hintze, 1972, 1978; Moore, 1973; Miller, 1982).

The pre-Lake Bonneville materials in the Bonneville basin are
significant to liquefaction potential only to the extent that they
provided the source of lake sediments. The pre-Lake Bonneville Materials
exposed around the margins of the lake within Utah County are not
particularly significant themselves because the currents in the lake
distributed widely all but the coarsest sediments.

Lake Bonneville Materials

Material Properties. These materials constitute the near-surface
sediments in most of the Bonneville basin below an elevation of about
5180 ft. (1580 m). This elevation is significant because it represents
the shore line created by the largest lake in the basin. The elevation
of the highest shore line varies considerably from place to place
within the basin because of differential isostatic rebound resulting
from loading and unloading of the earth's crust with the water impounded
by the lake. Tectonic deformations along fault zones also contribute
to the variation in elevation of shore lines.

The lake materials are principally silt. Varying amounts of sand,
gravel and clay are present with the coarsest fraction being found
closest to the mountain front and the finest being found in the central
part of the basin.

The lake sediments are commonly thinly bedded. Fine sand layers
are commonly present between clayey silt layers. Locally, thick layers
of sand are present in the basin. Very coarse sand and gravel are
commonly located where lake shore lines were once present.

It is important to note that substantially less sandy material was found in Utah County than in Davis County (Anderson and others, 1982) or Salt Lake County (Anderson and others, 1986). The reason for this is the generally finer-grained bedrock materials in the drainage areas of Utah County and the fact that Utah valley was a restricted arm of Lake Bonneville. Therefore, no major currents carried the clay and silt to the central part of the basin, leaving sandier material behind.

Age and Elevation of Lake Levels. Four principal lakes occupied the basin in latest Pleistocene time. The basin existed prior to late Pleistocene time and lacustrine sediments undoubtedly accumulated. Evidence for the existence of major lakes in this basin prior to latest Pleistocene time has been obscured by the younger lake deposits. Reinterpretation of evidence used by early workers to substantiate the existence of large lakes in the basin during early late Pleistocene time has recently been done (Scott, 1980; Currey and Oviatt, 1985). The basic conclusion is that the lake at the Bonneville level (elevation 5180 ft. (1580 m) was the largest of the Pleistocene lakes in the basin. Radiocarbon dates on materials collected from the highest beach deposits suggest that Lake Bonneville existed at this level during a period from about 16,000 to 15,000 years ago (Currey and Oviatt, 1985), with a possible brief period of lake lowering about 15,500 years ago.

A probable reason that no lakes as large as Bonneville existed prior to about 30,000 years ago is that the Bear River, which formerly flowed to the Snake River, was captured about that time by one of the drainages of the Bonneville basin. With the added volume of water from the Bear River, which drains part of the northern slope of the western Uinta Mountains, inflow greatly exceeded evaporation and the lake rose

to its maximum level controlled by topography at Red Rock Pass at the northern end of Cache Valley in Idaho.

Approximately 15,000 years ago, Lake Bonneville eroded a channel at Red Rock Pass. The erosion cut quickly through about 365 ft. (110 m) of weakly cemented materials and caused catastrophic flooding of the Snake River Plain (Currey, 1980, p. 74). A new threshold elevation of approximately 4815 ft. (1470 m) was established. The shore features associated with this threshold have been named the Provo shore line for distinctive features in Utah County. This shore line apparently was occupied from about 15,000 to 14,000 years ago (Currey and Oviatt, 1985, p. 19).

The climate of the basin controlled the lake levels after the Provo shore lines were formed. After 14,000 years ago, evaporation exceeded inflow and the lake dropped to an elevation below the floor of Utah Valley. Utah lake is the remnant of Lake Bonneville in Utah County.

Significance of Lake Environment. The ages of the lake levels are significant for the purpose of comparing the Utah County liquefaction potential analysis to published analyses of other areas. In general, Youd and Perkins (1978, p. 441) considered lacustrine deposits less than 500 years old to have high liquefaction susceptibility. They assigned moderate susceptibility to Holocene lacustrine sediments and Pleistocene lacustrine sediments were considered to have low liquefaction susceptibility.

The results of the current research on liquefaction potential of Utah County and the results from Davis County and Salt Lake County (Anderson and others, 1986) indicate that sediments deposited in late Pleistocene lakes are highly susceptible to liquefaction. This may

result from the restricted ground water lowering that can take place in closed basins. Sea level is the controlling plane for erosion and deposition in coastal areas, such as San Francisco, where much research has been done with respect to liquefaction potential. Lajoie and Helley (1975, p. 50) distinguished younger and older alluvial deposits on the basis of the sea level stand to which they are graded. Young deposits comprise alluvial fans being formed under existing hydrologic conditions; active streams in young deposits are graded to present sea level. Older alluvial deposits are partly covered by Holocene sediments and were formed by streams which were graded to lower stands of sea level during the late Pleistocene.

The significance of this observation is that late Pleistocene deposits in coastal areas were formed either when sea level was low (e.g., Oxygen Isotype Stage 2 or 6, Shackleton and Opdyke, 1973, p. 45) or deposits formed before the last low stand of sea level were drained and dissected during the last low stand. The 365 ft. (110 m) drop in sea level during Oxygen Isotype Stage 2 (approximately 17,000 years ago) would have a pronounced affect on sedimentation in coastal areas.

The age of the most recent low stand of sea level corresponds fairly well with the high stand of Lake Bonneville. This suggests that the large volume of water constituting glaciers on land masses at this time contributed not only to lower of sea level, but raising Lake Bonneville as well. Therefore, sediments were essentially being dewatered in coastal areas at the same time they were being deposited in Lake Bonneville. Consequently, ages of material relating to liquefaction potential on the basis of research done in coastal areas do not appear appropriate for internally-drained areas such as the Great Sale Lake basin.

Post-Lake Bonneville Materials

These materials have limited distribution in Utah County. Chiefly, they are present along the principal drainage channels entering the Valley from the surrounding mountains or leaving the valley along the Jordan River in the north part of the county. Relatively isolated alluvial and debris fans are scattered throughout the county.

Two large lateral spread landslides involving lake deposits have been mapped by Miller (1982). Only a few other landslides have been mapped in Utah County and these typically involve pre-lake materials. The notorious Thistle landslide is located in Utah County (Anderson and others, 1984). The lateral spread landslides are discussed later in this report on the section pertaining specifically to ground failures.

Post-Lake Bonneville materials have been mapped in Utah County by Bissell (1963), Hunt and other, (1954), Miller (1982), and Davis (1983). One of the most dominant processes responsible for deposition of post-Lake Bonneville materials is cloudburst and snowmelt floods (Marsell, 1972). Material deposited by cloudburst is relatively local in nature and typically situated near the mountain front as alluvial fans and debris fans. Large boulders can be carried by the floods which consist of viscous slurries of clay, silt and sand.

Most streams in Utah County drain small areas; the major exception to this is Spanish Fork which drains about 500 square miles. The major rock type is this drainage area is siltstone which contributes much fine-ground sediment to Utah Valley. Post-Lake Bonneville sediments are localized along stream channels and alluvial fans in the County.

Soil Development

In general, aside from local accumulations of alluvial fan, debris fan, and stream deposits, lacustrine materials in Utah County have been continuously exposed as lake levels dropped. The soil survey of the Utah Valley area prepared by Swenson and other (1972) was reviewed and found to be of limited value in interpreting liquefaction susceptibility. Youd and others (1979, p. 40) used relative development of pedogenic soil profiles to distinguish Holocene deposits which they considered to be more susceptible to liquefaction from Pleistocene deposits which they considered to be less susceptible. This approach was deemed unsatisfactory in Utah County because our knowledge of Lake history indicates that virtually all lake deposits in the county range in age from about 16,000 to about 14,000 years old. Therefore, mapping Holocene deposits would not provide a useful means of identifying liquefaction susceptibility.

Geotechnical Data

Available Subsurface Data

Soils considered to be susceptible to liquefaction are found virtually everywhere within the study area west of the Wasatch Mountains excluding West and Lake Mountains. Consequently, site specific analyses were required to delineate zones of differing liquefaction susceptibility. The necessary soil boring data required to perform a liquefaction analysis included accurate descriptions of the soil profiles, standard penetration resistance data, ground water depth and the grain size characteristics of granular layers. Such information was sought from existing records and supplemented by field and laboratory testing programs.

Soil boring data were obtained from various consulting firms and government agencies which had performed subsurface investigations within the study area. Numerous techniques had been used to obtain subsurface information. The standard penetration test was not used by all investigators to measure field densities and to obtain samples. Therefore, it was necessary to convert various (non-standard) penetration values to standard penetration blow count values so that the data could be used with the Seed and Idriss (1982) chart (Fig. 9). The energy conversion technique presented by Lowe and Zaccheo (1975) is shown on Fig. 11 and was used to convert non-standard data.

All existing data was then plotted on the Soils and Ground Water Data Map of the study area shown on Plates 2A through 2D. The data presented on this map consist of 1) the boring depth, 2) the location of liquefiable deposits, and 3) the depth to ground water.

Field Investigation

Locations for additional subsurface investigations in the study area were selected, based on lack of existing data in those areas, combined with the potential for future population growth. The subsurface investigation consisted of performing borings and cone penetration soundings. Permission was obtained from the landowners where each boring or cone penetration was to be performed.

During a three-week period, approximately 45 electric cone penetration tests (CPT) and 20 borings with standard penetration tests (SPT) were performed. The electric cone penetrometer is pushed at a constant rate downward through the soil deposit. The CPT electronically records the resistance at the cone tip and on the cone sleeve. The record was made on a strip chart recorder for both endbearing and sleeve resistance.

Sampler-Hammer Ratio, R_s, $\frac{ft^2}{lb}$, x 10^{-5}

4.0

2.0

$D_r = 20\%$

$D_r = 40\%$

$D_r = 70\%$

$D_r = 90\%$

Very Loose

Loose

Medium Dense

Dense

Very Dense

1.0

0.5

2   4   6   10   20   40   60   100   200

Driving Resistance, B, Blows/ft

Dames & Moore Type U Sampler

Reinard W. Brandley Type U Sampler

Standard Penetration 2" Split Spoon Sampler

Reinard W. Brandley Type G Sampler

$$R_s = \frac{D_o^3 - D_i^3}{144 \ WH}$$

D_o = Outside Diameter of Sampler, inches

D_i = Inside Diameter of Sampler, inches

W = Weight of Hammer, pounds

H = Height of Drop, inches
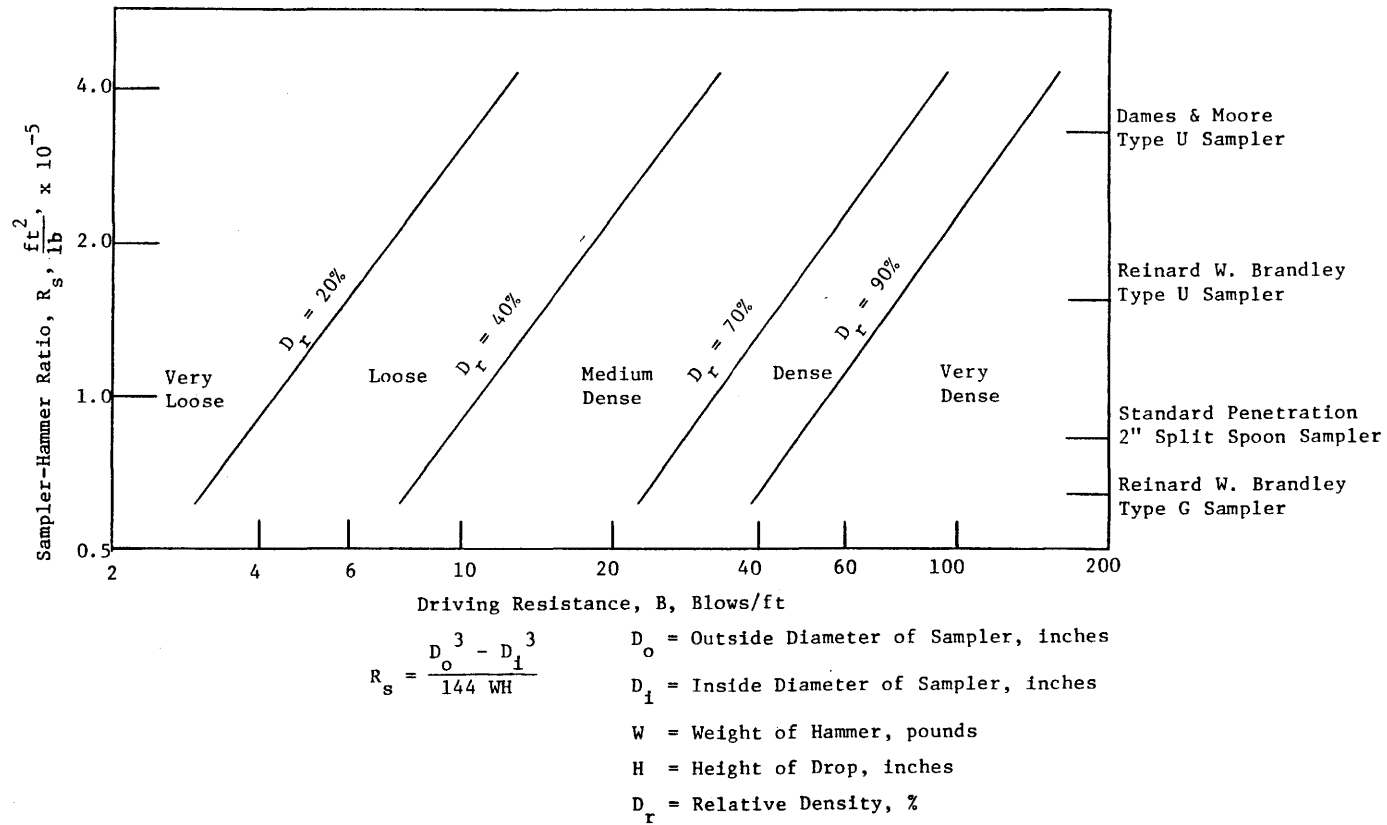
D_r = Relative Density, %

Figure 11. Penetration resistance conversion relationship for cohesionless sands and silts (after Lowe and Zacchoe, 1975)

After making a field inspection of the cone records, borings were performed about 4 feet away from selected cone penetration holes to provide correlation between the CPT results and soil type, and also correlation between cone penetration resistance and SPT values. Borings were also drilled in selected locations where the cone penetration met refusal at a shallow depth.

Hollow stem auger tools were used for drilling, and the standard penetration tests were performed using conventional methods (140 lb. hammer, dropping through 30"). Samples of soil were obtained using the standard split spoon sampler. Boring depths ranged from 20 to 40 feet.

The drill rig was easily adapted and able to push the electric cone penetrometer to depths ranging from 30 to 70 feet. A strip chart recorder provided a hard copy of the cone penetration record.

Laboratory work

The laboratory work consisted of making grain size analysis and the determination of Atterberg limits so that each field soil sample could be classified. About 90 soil samples were collected. These samples were tested and classified at the Utah State University Civil Engineering soils laboratory.

Soils and Ground Water Data Map

The Soils and Ground Water Data Map shown on Plates 2A through 2D was prepared to summarize the aerial extent and vertical depth of the liquefiable soil deposits and the ground water conditions in Utah County. The soils and ground water data include:

1. Depths at which liquefiable layers exist

2. Depth to ground water

Ground water contour lines showing zones of various depths to first ground water have been drawn on the map. As shown on Plates 2A through 2D, a letter designation was used to show the range of water table depths.

Existing Ground Failure

Introduction

Ground failures involving the lake deposits exist in two locations of Utah County as shown on the Selected Geologic Data Map, Plates 1A through 1D. These two failures have been interpreted as "lateral spread" failures induced by earthquake shaking by Miller (1982). Other ground failures in the county appear to be simply "landslides" which are not necessarily caused by earthquake shaking. However, earthquake activity could have played a role in the timing of such landslides.

Lateral Spread Failures

Lateral spread failures have been identified by Miller (1982). These failures are shown on Plate C located below an elevation of 4600 ft. (1400 m). These areas are characterized by ground slopes ranging from 0.5 to 5.0 percent. Slopes of this range are considered to be susceptible to the lateral spread process during liquefaction events.

Other Ground Failures

A few other landslides have been mapped in Utah County by Miller (1982). Earthquake shaking could have played a significant role in initiating the landslides. However, these landslides could be static failures related simply to lowering of lake levels. Down-cutting of streams in response to lower lake levels could also tend to created oversteepened slope conditions which promote instability.

Ground Slope Data

As discussed earlier, the major types of ground failure which result from earthquake-induced liquefaction include flow landslides, lateral spreading landslides, and loss of bearing capacity. Youd (1978) suggests that the type of ground failure induced by liquefaction is related to the ground surface slope. A letter designation was used on Plates 3A through 3D, Ground Slope and Critical Acceleration Map, to show the range of slopes which may be used to predict the type of failure that might occur. The ground slope ranges shown on Plates 3A through 3D were estimated from U.S. Geological Survey topographic quadrangles.

LIQUEFACTION POTENTIAL

Critical Acceleration as a Liquefaction Potential Indicator

Critical accelerations computed for specific sites within the study area were assigned liquefaction potential classifications according to the probability that the critical acceleration would be exceeded during the next 100 years. The liquefaction potential and the corresponding exceedance probabilities were discussed earlier and presented in Table 2.

A seismic risk study was performed by Dames and Moore (1976) for the Orem area and Figure 12 shows the probability of exceedance curve of maximum earthquake accelerations in 100 years. This curve was plotted with several other curves that have been generated along the Wasatch Front and was found to be about the average of all the curves, therefore, it was decided the Orem curve was representative of Utah County. Table 4 summarizes the exceedance probability data.
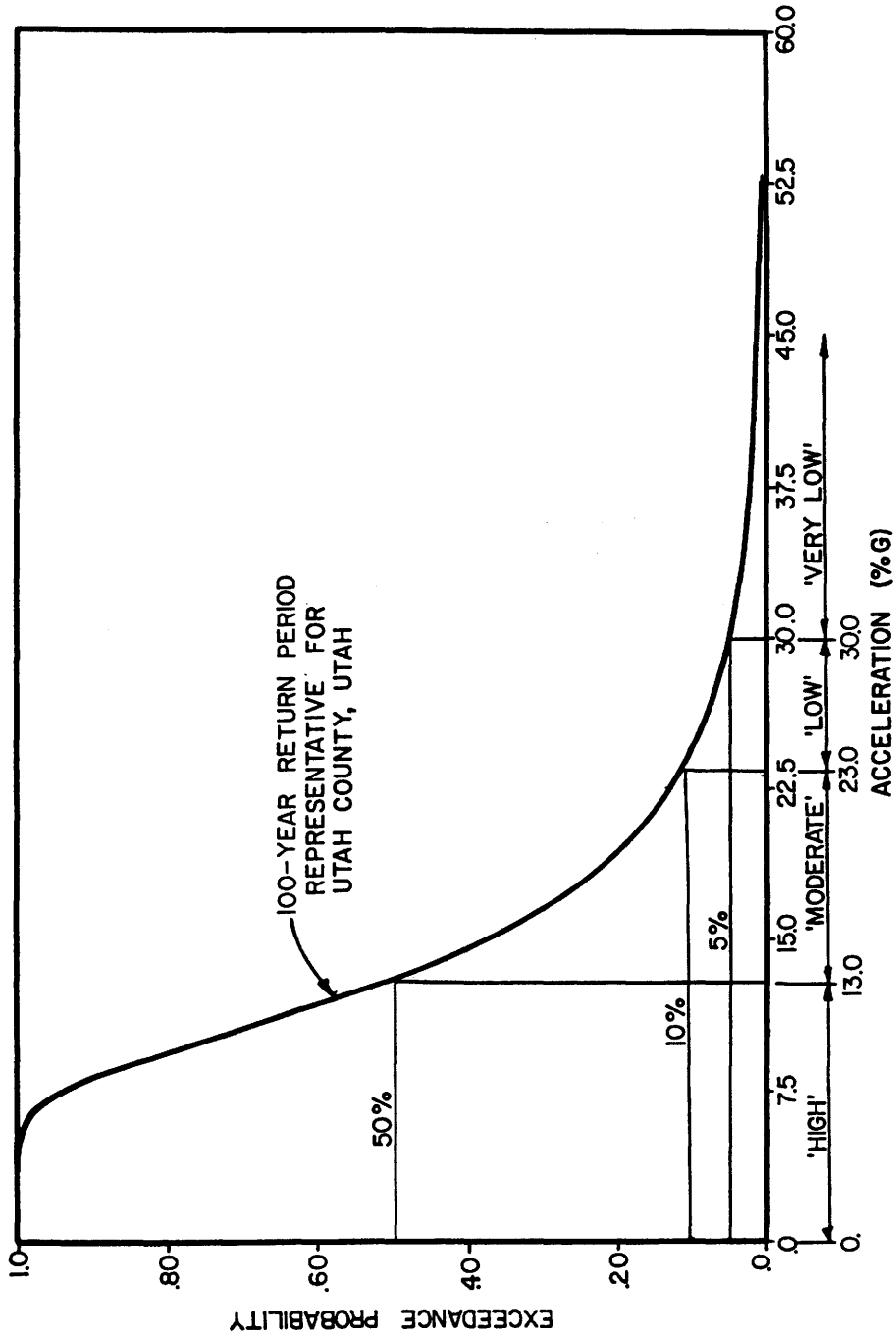
Figure 12. Probability of exceedence curve for maximum earthquake accelerations.

Table 4. Liquefaction potential related to critical
acceleration. (From Dames & Moore, 1978)

Liquefaction Potential	Critical Acceleration	Approximate 100 year Exceedance Probability
High	< 0.13 g	> 50%
Moderate	0.13 - 0.23 g	50 - 10%
Low	0.23 - 0.30 g	10 - 5%
Very Low	> 0.30 g	< 5%

Symbols were used to illustrate accelerations on the Critical Acceleration Map on Plates 3A through 3D. The symbols are keyed in the explanation on the plates.

The method of evaluating liquefaction potential in this study is based primarily on the results of the standard penetration test which measures the resistance a soil exhibits to driving a standard sampler one foot. Therefore, a critical acceleration value could not be assigned to sand layers less than one foot thick.

Liquefaction Potential Map

The Liquefaction Potential Map developed for the Utah County study area is shown on Plates 4A through 4D. Liquefaction potential has been classified as high, moderate, low and very low depending on the probability that the critical acceleration will be exceeded in 100 years. As previously discussed, the probable types of ground failure may be predicted by using the Liquefaction Potential Map in conjunction with the Ground Slope Map and the Soils and Ground Water Data Map.

A general summary of the liquefaction potential of Utah County can be made with reference to the ground surface elevations. Generally, the areas most susceptible to liquefaction are below an elevation of about

4550 ft. The areas with a liquefaction potential classification of
very low are located at the higher elevations of the study area as shown
on the Liquefaction Potential Map, Plates 4A through 4D.

CONCLUSIONS AND RECOMMENDATIONS

Ground failure caused by liquefaction is a primary hazard associated
with earthquakes. The first step in avoiding this hazard is to recognize
where liquefaction might occur. A Liquefaction Potential Map has been
compiled for Utah County, Utah showing areas where conditions are favorable
for liquefaction to occur.

Fine sand and silty sand are the soil types most conductive to
liquefaction and they are found throughout the Utah County study area.
Soil type alone, however, does not determine the liquefaction potential
of a given site. Several important factors influencing liquefaction
potential were considered in this study. The standard penetration test
provided a useful means for evaluating the influence of the soil structure,
previous seismic history, and age of the deposit as well as the relative
density of the soil. An increase in the resistance to liquefaction
from any of these factors is reflected by a corresponding increase in
the standard penetration resistance.

The standard penetration resistance along with limited cone
penetration resistance was used to compute the ground surface acceleration
that would be required to induce liquefaction (critical acceleration).
The liquefaction potential was then assigned on the basis of the
probability that the critical acceleration would be exceeded in 100
years. Local geologic conditions were also considered in refining
liquefaction potential boundaries.

The information generated by this study should prove to be valuable for those concerned with future land development. Planners and other concerned parties should realize that areas showing a high liquefaction potential need not be ruled out as possible sites for construction. However, we believe further analyses should be required for these sites including an economic analysis of preventive or protective measures that can be used to reduce the liquefaction potential. Haldar (1980) has developed a decision analysis framework which considers both the technical and economic aspects of limiting or eliminating damage associated with liquefaction. Anderson and Keaton (1986) have presented a decision matrix that relates potential mitigation measures to the liquefaction potential and the proposed land use.

One problem often encountered during this study was how to assess the susceptibility of thin sand layers and lenses. Since the standard penetration test primarily was used as a basis for this study, reliable data could only be obtained for sand strata greater than one foot thick. Damages associated with the liquefaction of thin sand layers and lenses are not uncommon (Seed, 1968) but an accurate means for identifying the relative density of such strata has not been developed. The cone penetrometer provides a direct means for continuously identifying liquefaction susceptibility in a soil profile and was used on a limited basis in this study. The cone penetrometer offers an economical means of providing continuous subsurface profiles, however, the validity of the data is still somewhat questionable because of the relatively small amount of correlation data between the cone penetrometer and soil liquefaction characteristics (Seed and others, 1983).

It is recommended that the liquefaction potential map be updated continually as more soil boring information becomes available and as new and improved techniques are developed for analyzing liquefaction.

LIST OF REFERENCES

Algermissen, S.T., and D.M. Perkins. 1972. A technique for seismic
    zoning: general considerations and parameters: Proc. Int'l
    Conference on Microzonation, Seattle, Washington, p. 865-878.

Anderson, L.R., J.R. Keaton, K. Aubry, and S.J. Ellis. 1982. Lique-
    faction Potential Map for Davis County, Utah. Final report to the
    U.S. Geological Survey by Utah State University. Contract No.
    14-08-0001-19127.

Anderson, L.R., J.R. Keaton, T.F. Saarineen, and W.G. Wells, II. 1984.
    The Utah Landslides, Debris Flows, and Floods of May and June
    1983. Committee on Natural Disasters, Commission on Engineering
    and Technical Systems, National Research Council.

Anderson, L.R., J.R. Keaton, A.C. Allen, and J.E. Spitzley. 1986.
    Liquefaction Potential Map for Salt Lake County, Utah. Final
    report to the U.S. Geological Survey by Utah State University.
    Contract No. 14-08-0001-19910.

Anderson, L.W. and D.G. Miller. 1979. Quaternary Faulting in Utah:
    In Proceedings of Conference X, Earthquake Hazards Along the
    Wasatch and Sierra-Nevada Frontal Fault Zones, National Earthquake
    Hazards Reduction Program, 29 July - 1 August, 1979. U.S. Geological
    Survey Openfile report 80-801, p. 194-226.

Arabasz, Walter J., R.B. Smith and W.D. Richins. 1979. Earthquake
    Studies in Utah, 1850-1978. University of Utah Seismograph Stations,
    Department of Geology and Geophysics, University of Utah, Salt
    Lake City, Utah.

Baker, A.A. 1964. Geologic map of the Orem quadrangle, Utah: U.S.
    Geological Survey Geologic Quadrangle Map GQ-241, scale 1:24,000.

Baker, A.A. 1972. Geologic map of the Bridal Veil Falls quadrangle,
    Utah: U.S. Geological Survey Geologic Quadrangle Map GQ-998,
    scale 1:24,000.

Baker, A.A. 1973. Geologic map of the Springville quadrangle, Utah
    County, Utah: U.S. Geological Survey Geologic Quadrangle Map GQ-
    1103, scale 1:24,000.

Baker, A.A. and M.D. Crittenden, Jr. 1961. Geology of the Timpanogos
    Cave, Utah: U.S. Geological Survey Geologic Quandrangle Map-132,
    scale 1:24,000

Baligh, M.M., V. Vivatrat and C.C. Ladd. 1980. Cone penetration in
    soil profiling. Journal of the Geotechnical Engineering Division,
    ASCE, Vol. 106, No. GT4, Proc. Paper 15377, April. p. 447-461.

Bischoff, J.E. 1985. Liquefaction Potential Mapping of Utah County,
    Utah. M.S. Thesis, Utah State University Library, Logan, Utah.

Bissell, H.J. 1963. Lake Bonneville--Geology of Southern Utah Valley, Utah: U.S. Geological Survey Professional Paper 257-B, p. 101-130.

Coffman, J.L. and C.A. von Hake. 1973. Earthquake history of the United States: National Oceanic and Atmospheric Administration, publication 41-1.

Cook, K.L. and J.W. Berg, Jr. 1961. Regional gravity survey along the central and southern Wasatch Front, Utah: U.S. Geological Survey Professional Paper 316-E, p. 75-89, 1 Plate.

Currey, D.R. and C.G. Oviatt. 1985. Durations, average rates, and probable causes of Lake Bonneville expansions, still stands, and contractions during the last deep-lake cycle, 32,000 to 10,000 years ago: in Kay, P.A. and Diaz, H.F., eds. Problem of and prospects for predicting Great Salt Lake levels, Conference Proceedings, Center for Public Affairs and Adminstration, University of Utah, p. 9-24.

Dames and Moore, 1976. Seismic Risk Study report. Proposal for Utah Valley water purification plant, Orem, Utah. 27 p.

Dames and Moore. 1978. Final report, Development of criteria seismic risk mapping in Utah, for State of Utah Department of Natural Resources Seismic Safety Advisory Council. Unpublished Consultants Report. July 20. 14 p.

Davis, F.D. 1983. Geologic Map of the Southern Wasatch Front, Utah: Utah Geological and Mineral Survey, Map 55-A.

Douglas, Bruce J., Richard S. Olsen, and Geoffrey R. Mortin. 1981. Evaluation of cone penetromter test for SPT liquefaction assessment, ASCE, Preprint 81-544.

Gibbs, H.J. and W.G. Holtz. 1957. Research on determining the density of sands by spoon penetration testing. Proceedings of the 4th International Conference on Soil Mechanics and Foundation Engineering. London.

Haldar, A. 1980. Liquefaction study - a decision analysis framework. Journal of the Geotechnical Engineering Division, ASCE, Vol. 106, No. GT12m Proc. paper 15925. December. p. 1297-1312.

Hely, A.G., R.W. Mower, and C.A. Harr. 1971. Water Resources of Salt Lake County, Utah: Utah Department of Natural Resources Technical Publication No. 31, 244 p.

Hill, R.J. 1979. A liquefaction potential map for Cache Valley, Utah. Unpublished M.S. thesis. Utah State University Library, Logan, Utah.

Hintze, L.F. 1972. Wasatch Fault zone east of Provo, Utah, in Environmental geology of the Wasatch Front, 1971: Utah Geological Association Publication 1, p. F1-F10.

Hintze, L.F. 1978. Geologic map of the Y Mountain area, east of Provo, Utah: Brigham Young University Geology Studies, Special Publication 5, map scale 1:24,000.

Hunt, C.B., H.D. Varnes and H.E. Thomas. 1953 [1954]. Lake Bonneville-- Geology of northern Utah Valley, Utah: U.S. Geological Survey Professional Paper 257-A, 99 p.

Lajoie, K.R. and E.J. Helley, 1975. Differentiation of sedimentary deposits for purposes of seismic zonation: in Borcherdt, R.D., ed., Studies for seismic zonation of the San Francisco Bay Region, U.S. Geological Survey, Professional Paper 941-A, p. 39-51.

Lowe, John and Philip Zaccheo. 1975. Subsurface explorations and sampling. Chapter 1 of Foundation Engineering Handbook, Hans F. Winterkorn and Hsai-Yang, Eds. Van Nostrand Reinhold Co., New York, New York. p. 1-66.

Marsell, R.E. 1972. Cloudburst and snowmelt floods, in Environmental geology along the Wasatch Front, 1971: Utah Geological Association Publication 1, p. N1-N28.

Miller, R.D. 1982. Surficial geologic map along the southern part of the Wasatch Front, Great Salt Lake, and Utah Valley, Utah: U.S. Geological Survey Map MF-1477.

Moore, W.J. 1973. Preliminary geologic map of western Traverse Mountains and northern Lake Mountains, Salt Lake and Utah Counties, Utah: U.S. Geologic Survey Miscellaneous Field Studies Map MF-490, scale 1:24,000.

National Research Council. 1985. Liquefaction of soils during earthquakes. Committee on Earthquake Engineering, Commission on Engineering and Technical Systems, National Research Council. National Academy Press, Washington D.C. Report No. CETS-EE-001.

Nichols, D.R. and J.M. Buchanan-Banks. 1974. Seismic hazards and land-use planning: U.S. Geological Survey Circular 690.

Peck, R.B., W.E. Hanson and T.H. Thornburn. 1974. Foundation engineering, second edition. John Wiley and Sons, Inc., New York. 514 p.

Schmertmann, J.H. 1978. Study of feasibility of using Wissa-type piezometer probe to identify liquefaction potential of saturated fine sands. Technical Report S-78-2, U.S. Army Engineer Waterways Experiment station. February. 73 p.

Scott, W.E. 1980. New interpretations of Lake Bonneville stratigraphy and their significance for studies of earthquake hazard assessment along the Wasatch Front: Proceedings of Conference X, Earthquake Hazards along the Wasatch and Sierra-Nevada Frontal Fault Zones, National Earthquake Hazards Reduction Program, 29 July - 1 August 1979, U.S. Geological Survey Openfile report 80-801, p. 548-576.

Seed, H.B. 1968. Landslides during earthquakes due to soil liquefaction. Journal of the Soil Mechanics and Foundations Division, ASCE, Vol. 93, No. SM5, Proc. Paper 6110. September. p. 1053-1122.

Seed, H.B. 1975. Earthquake effects on soil foundation systems. Chapter 25 of Foundation Engineering Handbook, Hans F. Winterkorn and Hsai-Yang Fang, Eds. Van Nostrand Reinhold Co., New York, New York. p. 700-732.

Seed, H.B. 1976. Evaluation of soil liquefaction effects on level ground during earthquakes. Preprint 2752, State-Of-The-Art Paper, ASCE Annual Convention and Exposition, Philadelphia, Pennsylvania. September 27 - October 1.

Seed, H.B. 1979. Soil liquefaction and cyclic mobility for level ground during earthquakes. Journal of the Geotechnical Engineering Division, ASCE, Vol. 105, No. GT2, Proc. Paper 14380. February. p. 201-255.

Seed, H.B. and I.M. Idriss. 1982. Ground motions and soil liquefaction during earthquakes. Volume 5. The Earthquake Engineering Research Institute, 2620 Telegraph Avenue, Berkeley, California. 134 p.

Seed, H.B., I.M. Idriss, and Ignacio Arango. 1983. Evaluation of liquefaction potential using field performance data. Proceedings Paper 17785. Journal of the Geotechnical Engineering Division, ASCE, 109(GT3):458-482.

Seed, H.B., K. Mori and C.K. Chan. 1977. Influence of seismic history on liquefaction of sands. Journal of The Geotechnical Engineering Division, ASCE, Vol. 103, No. GT4, Proc. Paper 12841. April. p. 257-270.

Seed, H.B. and W.H. Peacock. 1971. Test procedures for measuring soil liquefaction characteristics. Journal of the Soil Mechanics and Foundations Division, ASCE; Vol. 97, No. SM8, Proc. Paper 8300. August.

Shackleton, N.J. and N.D. Opdyke. 1973. Oxygen isotype and paleomagnetic stratigraphy of Equatorial Pacific core V28-238: oxygen isotype temperatures and ice volumes on a 10^5-year and 10^6-year scale: Quaternary Research Vol. 3, p. 39-55.

Swenson, J.L., W.M. Archer, K.M. Donaldson, J.I. Shiozaki, J.H. Broderick, and Lowell Woodward. 1972. Soil Survey of Utah County, Utah--Central Part: U.S. Department of Agriculture Soil Conservation Service, 161 p. and 32 maps, scale 1:20,000.

Tatsuoka, F., T. Iwasaki, K. Tokida, S. Yasuda, M. Hirose, T. Imai, and M. Kon-no. 1980. Standard penetration tests and soil liquefaction potential evaluation. Soils and Foundations. Japanese Society of Soil Mechanics and Foundation Engineering. 20(4).

Van Horn, Richard, J.L. Baer, and E.F. Pashley, Jr. 1972. Landslides along the Wasatch Front, Utah, in Environmental geology of the Wasatch Front, 1971: Utah Geological Association Publication 1, p. J1-J-16.

Youd, T.L. 1978. Major cause of earthquake damage is ground failure. Civil Engineering, ASCE, Volume 48, No. 4, April. p. 47-51.

Youd, T.L. 1981. Engineer, U.S. Geological Survey, Menlo Park, California, personal communication.

Youd, T.L. and S.N. Hoose. 1977. Liquefaction susceptibility and geologic setting. Proceedings of the 6th World Conference on Earthquake Engineering, New Delhi, India. January 10-14.

Youd, T.L. and David M. Perkins. 1978. Mapping liquefaction-induced ground failure potential. Journal of the Geotechnical Engineering Division, ASCE. 104(GT4):433-446.

Youd, T.L., D.R. Nichols, E.J. Helley and K.R. Lajoie. 1975. Liquefaction potential: in Borcherdt, R.D., ed., Studies for seismic zonation of the San Francisco Bay Region, U.S. Geological Survey Professional Paper 941-A, p. A68-A74.

Youd, T.L., J.C. Tinsley, O.M. Perkins, E.J. King, and R.F. Preston. 1979. Liquefaction Potential Map on San Fernando Valley, California: in Brabb, E.E., ed., Progress on Seismic Zonation in the San Francisco Bay Region: U.S. Geological Survey Circular 807, p. 37-48.